Power scale-up and propagation evolution of structured laser beams concentrated on 3D Lissajous parametric surfaces

2014 Laser Phys. Lett. 11 125806

(http://iopscience.iop.org/1612-202X/11/12/125806)

IOP Publishing | Astro Ltd
Laser Physics Letters
Laser Phys. Lett. **11** (2014) 125806 (6pp)
doi:10.1088/1612-2011/11/12/125806

Power scale-up and propagation evolution of structured laser beams concentrated on 3D Lissajous parametric surfaces

J C Tung[1], H C Liang[2], Y C Lin[1], K W Su[1], K F Huang[1] and Y F Chen[1,3]

[1] Department of Electrophysics, National Chiao Tung University, 1001 Ta-Hsueh Road Hsinchu 30010, Taiwan
[2] Institute of Optoelectronic Science, National Taiwan Ocean University, Keelung 20224, Taiwan
[3] Department of Electronics Engineering, National Chiao Tung University, 1001 Ta-Hsueh Road Hsinchu 30010, Taiwan

E-mail: yfchen@cc.nctu.edu.tw

Received 20 February 2014
Accepted for publication 3 October 2014
Published 30 October 2014

Abstract

We systematically explore the power scale-up and propagation evolution of Lissajous structured beams in a lowly Nd-doped YVO_4 laser with the off-axis pumping scheme. We experimentally found that the average output power can be up to 1.0 W for the output transmission in the range of 1.8–10% at an incident pump power of 6.2 W. It is also found that when the output transmission is greater than 5%, the spatial coherence is considerably reduced to lead to a feature of broken Lissajous figures in transverse patterns. Moreover, transverse patterns varying with propagation direction are remarkably measured to manifest the 3D characteristics of Lissajous structured beams. We also employ the formula of coherent states to make a comparison with experimental observations and to reveal the transverse momentum density varying with propagation direction.

Keywords: laser modes, structured beams, Lissajous figures, orbital angular momentum

(Some figures may appear in colour only in the online journal)

1. Introduction

Early in 1965, Herriott and Schulte [1] firstly found that an optical path can be folded between a pair of spherical mirrors to reveal a Lissajous pattern with spots on each mirror due to one or both of astigmatic reflecting surfaces. In 2003, it was demonstrate that the transverse patterns localized on the Lissajous figures could be directly generated in a Nd:YVO_4 laser with a doughnut-shape pumped profile [2, 3]. Lately, the off-axis pumping scheme was employed to systematically generate a variety of Lissajous structured beams in a Nd:YVO_4 laser with degenerate cavities. Lissajous structured beams are three-dimensional (3D) coherent waves to be concentrated on Lissajous parametric surfaces that are formed by the Lissajous curves with the relative phase varying in the longitudinal direction [4, 5]. Furthermore, it was theoretically verified that the Lissajous structured beam could be expressed as a coherent superposition of different Hermite–Gaussian modes which are degenerate with different longitudinal modes in the degenerate cavity. The mathematical form for Lissajous parametric surfaces is derived as [4]:

$$\begin{aligned} x(\vartheta, z) &= \sqrt{m_o}\, w(z) \cos\left[q\vartheta - \frac{\phi(z)}{p}\right]; \\ y(\vartheta, z) &= \sqrt{n_o}\, w(z) \cos(p\vartheta), \end{aligned} \tag{1}$$

where $0 \le \vartheta \le 2\pi$, $-\infty \le z \le \infty$, $\varphi(z) = (q + p)\theta_G(z) + \phi_o$, $\theta_G(z) = \tan^{-1}(z / z_R)$ is the Gouy phase, ϕ_o is the phase factor related to the transverse patterns in the beam waist and far-field region, $z_R = \sqrt{L(R-L)}$ is the Rayleigh range, R is the radius of curvature of the concave mirror, L is the cavity length, $w(z) = w_o\sqrt{1 + (z / z_R)^2}$, $w_o = \sqrt{\lambda z_R / \pi}$ is the beam radius at the waist, λ is the emission wavelength, m_o and n_o are the order indices, and p and q are integers. Figure 1 depicts an example described in equation (1) in the range between $z = -3L$ and $z = 3L$ for the case of $(p, q) = (1, 3)$ and $\phi_o = 0$.

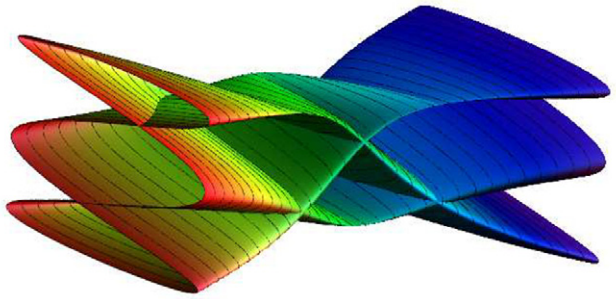

Figure 1. An example for the Lissajous parametric surface described in equation (1) for the range from $z = -3L$ to $z = 3L$ with $(p, q) = (1, 3)$, and $\phi_o = 0$.

On the other hand, it is well known that Hermite–Gaussian modes can be one-to-one transformed into Laguerre–Gaussian modes by use of a $\pi/2$-cylindrical-lens mode converter. With this conversion, Lissajous structured beams have been successfully transformed into so-called trochoidal structured beams that possess optical orbital angular momentum (OAM) [6–8]. Numerous researches on OAM of light have been exploited in a variety of applications, such as trapping [9, 10] and rotating [11] of microscopic particles in hydrodynamics and biology, controlling the chirality of twisted metal nanostructures [12, 13], quantum communication [14, 15], and spiral interferometry [16]. The scalability of the output power is an important issue for structured laser beams to be practically useful in most practical applications. Even though Lissajous structured beams have several intriguing characteristics for potential applications, the power scale-up for these beams has not been achieved so far.

In this article we explore the power scale-up of Lissajous structured beams in a lowly Nd-doped YVO_4 laser with the off-axis pumping scheme. We investigate the influence of the output transmission T_{oc} on the output performance of Lissajous structured beams. It is experimentally found that the average output power can generally exceed 1.0 W for T_{oc} in the range of 1.8–10% at an incident pump power of 6.2 W. Nevertheless, experimental results also reveal that when T_{oc} is greater than 5%, the spatial coherence is conspicuously reduced and the transverse patterns start to display a feature of broken Lissajous figures. Considering the output efficiency and the spatial coherence, the optimal values for T_{oc} are in the range of 1.8–5.0%. Furthermore, we control the exposure time of the beam profiler to capture the transverse images varying with propagation direction for manifesting the 3D characteristics of Lissajous structured beams. Finally, we exploit the formula of coherent states [17] and perform numerical calculations to reveal the transverse momentum density of Lissajous structured beams varying with propagation direction. It is believed that the accomplishment of watt-level average output power can effectively enhance the feasibility of utilizing Lissajous structured beams for practical applications.

2. Experimental setup

Figure 2 shows the experimental setup for generating a variety of Lissajous structured beams in a $Nd:YVO_4$ laser with the off-axis pumping scheme in concave-plano degenerate cavities. The gain medium was an *a*-cut 0.2 at.% $Nd^{3+}:YVO_4$ crystal with a length of 10 mm and a cross section of $3 \times 3\,mm^2$. Note that highly Nd-doped gain media were used in earlier studies to obtain low threshold. On the contrary, lowly Nd-doped gain media were usually employed to scale the output power for avoiding the thermally induced fracture [18]. Both end surfaces of the $Nd:YVO_4$ crystal were coated for anti-reflection at 1064 nm ($R < 0.2\%$) and wedged at 0.2° to suppress the Fabry–Perot etalon effect. The gain crystal was wrapped with indium foil and mounted in a water-cooled copper holder. The water temperature was maintained approximately at 16 °C to obtain a stable operation. Since generating super-high order transverse modes is indispensible for achieving Lissajous structured beams, a smaller radius-of-curvature of the concave cavity mirror is of great benefit to the generation of super-high order modes for a fixed off-axis pumping. Nevertheless, the radius-of-curvature of the concave mirror needs to match the cavity length that is constricted by the length of the gain medium. As a result, the radius-of-curvature of the concave mirror was chosen to be 30 mm. The input concave mirror was coated for anti-reflection ($R < 0.2\%$) at 808 nm on the entrance face and was coated for high reflection ($R > 99.8\%$) at 1064 nm and high transmission ($T > 95\%$) at 808 nm on the concave surface. Several flat output couplers with different output transmissions in the range of $0.4\% < T_{oc} < 25.0\%$ at 1064 nm were used to explore the influence of the output coupling on the lasing performance. The pump source was an 808 nm fiber-coupled laser diode with a core diameter of 200 µm, a numerical aperture of 0.22, and a maximum output power of 7.5 W. A focusing lens with 25 mm focal length and 85% coupling efficiency was used to focus the pump beam into the laser crystal. The average pump radius was estimated to be approximately 110 µm. Even though larger displacements for the off-axis pumping ideally lead to higher transverse orders, the size of gain medium and the diffraction loss constrict the available displacements. Consequently, the displacements for the off-axis pumping for the present experiment were set to be $\Delta x = 0.9$ mm and $\Delta y = 0.6$ mm in the x and y directions, respectively.

3. Experimental results and analyses

First of all, the cavity length was set to be 14.7 mm for obtaining the Lissajous structured beams with $(p, q) = (3, 1)$. Figure 3 depicts the dependences of the average output power and the far-field transverse pattern on the output transmission for several incident pump powers. It can be seen that the optimum T_{oc} is approximately 98% for the incident pump power less than 4.85 W. On the other hand, the average output power can generally exceed 1.0 W for T_{oc} in the range of 1.8–10% at an incident pump power of 6.2 W. However, high output coupling may significantly decrease the spatial coherence. As seen in figure 3, high output coupling leads to a broken feature in far-field transverse patterns for T_{oc} greater than 5%. As a result, the optimal values for T_{oc} are approximately in the range of 1.8–5.0% by considering the output efficiency and the spatial coherence.

We then used the output coupler with $T_{oc} = 1.8\%$ to generate various Lissajous structured beams with different indices

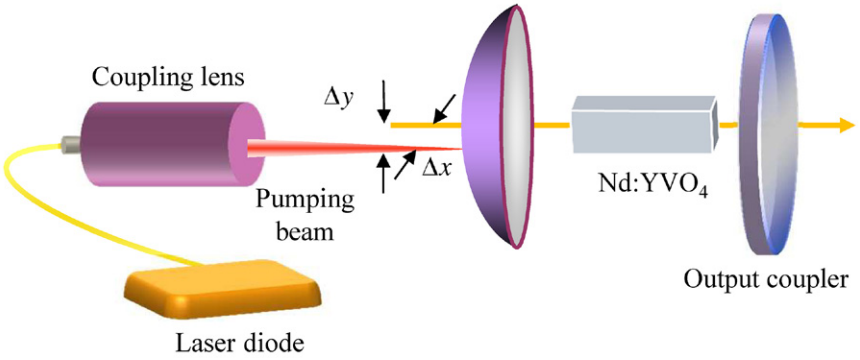

Figure 2. Experimental setup for generating a variety of Lissajous structured beams in a $Nd:YVO_4$ laser with the off-axis pumping scheme in concave-plano degenerate cavities.

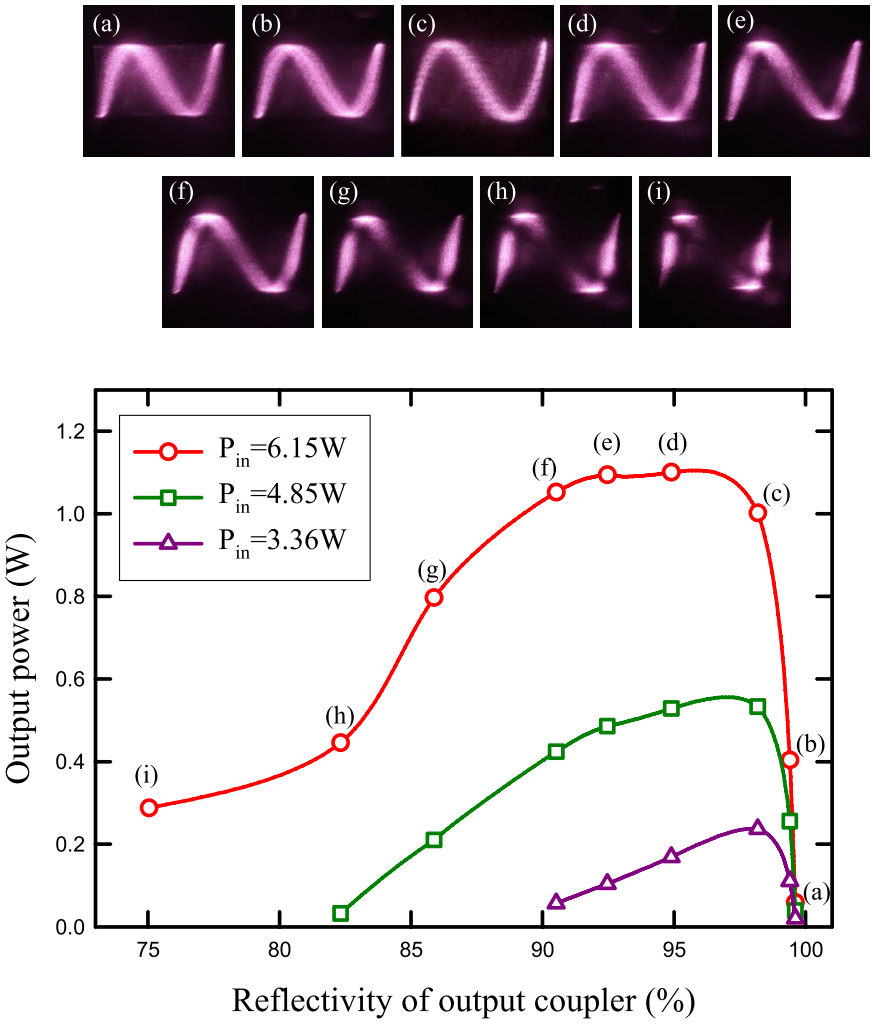

Figure 3. Experimental results for the dependences of the average output power and the far-field transverse pattern on the output transmission for several incident pump powers for the case of $(p, q) = (3, 1)$.

(p, q) for the cavity length in the range of 13.8–16.3 mm. Figure 4 shows experimental results for the average output powers and the far-field transverse patterns for numerous degenerate cavity lengths at an incident pump power of 6.2 W. It can be seen that the average output powers for different Lissajous structured beams are nearly to be constant and can be generally up to 1 W. To manifest 3D characteristics of Lissajous structured beams, we properly control the exposure time of the beam profiler to selectively capture the transverse images varying with propagation direction. Figure 5 depicts experimental results for displaying 3D features of Lissajous structured beams corresponding to the far-field patterns shown in figure 4. The propagation evolution of the transverse patterns can be clearly seen. To the best of our knowledge, it is an intriguing approach to exhibit spatial characteristics of 3D optical coherent waves.

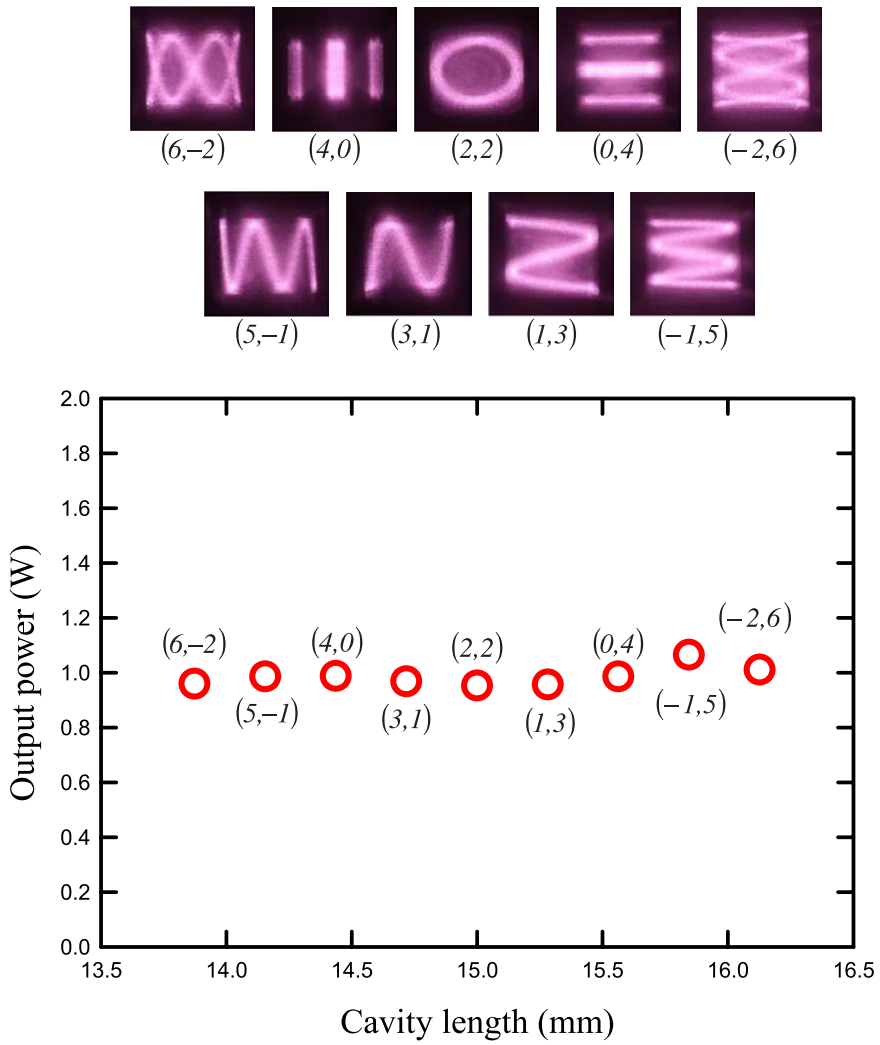

Figure 4. Experimental results for the average output powers and the far-field transverse patterns for numerous degenerate cavity lengths at an incident pump power of 6.2 W.

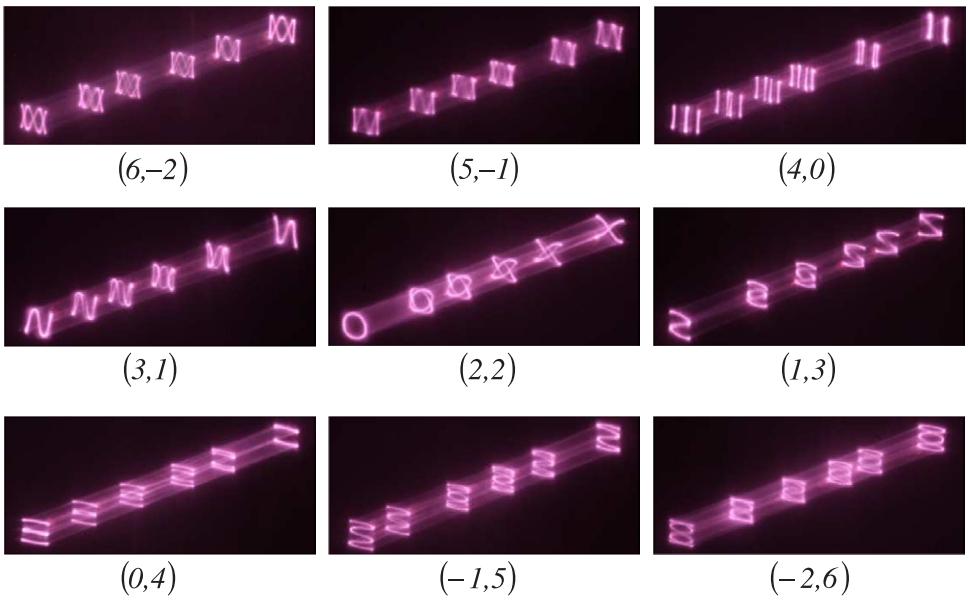

Figure 5. Experimental results for displaying 3D features of Lissajous structured beams corresponding to the far-field patterns shown in figure 4.

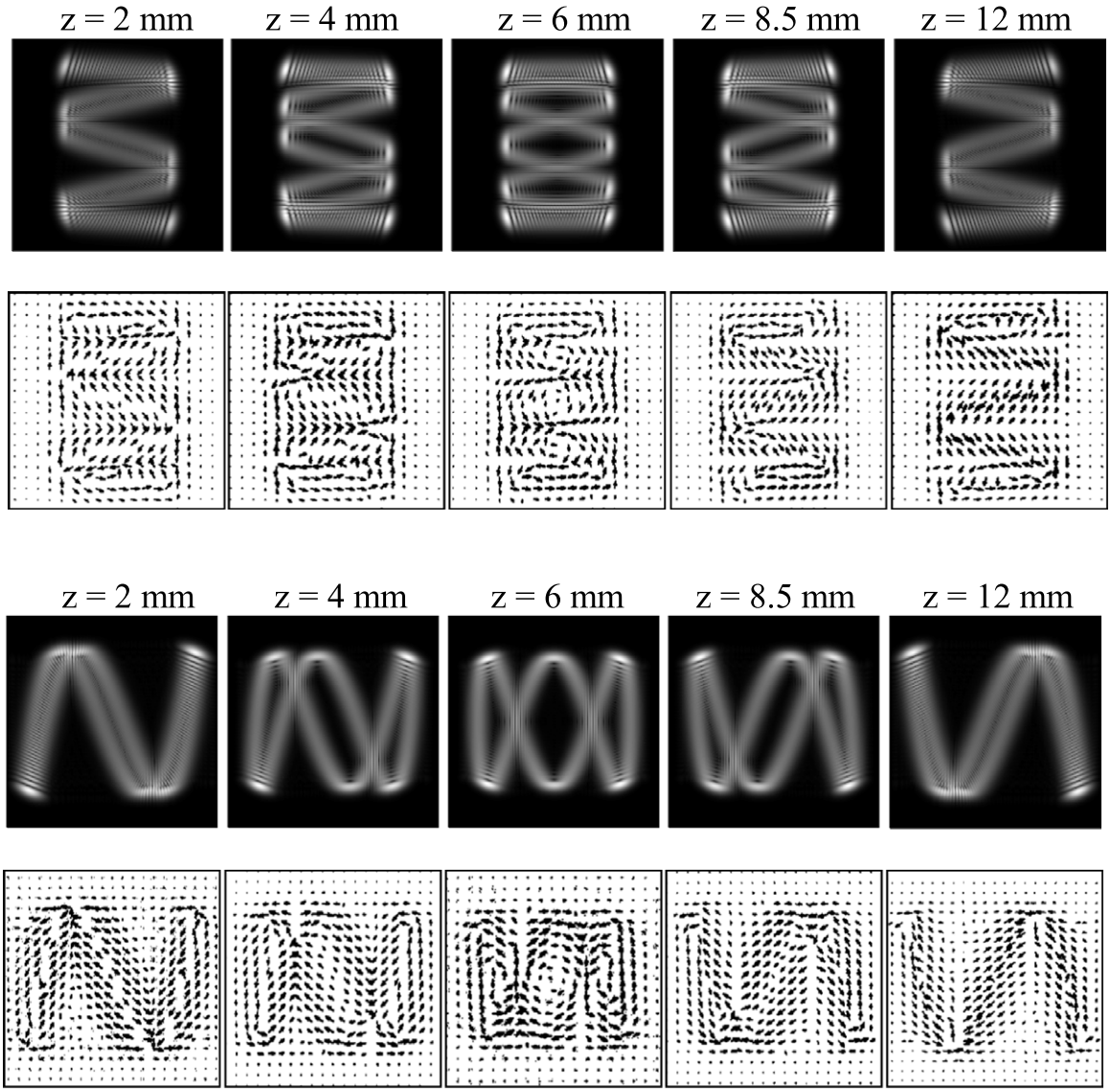

Figure 6. Calculated results for transverse patterns and transverse momentum densities varying with propagation direction from $z = 2$ mm to $z = 2$ mm for the cases of $(p, q) = (-1, 5)$ in the first and second rows and $(p, q) = (3, 1)$ in the third and fourth rows.

Next we perform numerical calculations to manifest the transverse momentum density of Lissajous structured beams varying with propagation direction. With the formula of quantum coherent states [17], the wave function for Lissajous structured beams is given by

$$\Psi^{p,q,s}_{m_o,n_o,l_o}(x,y,z) = \frac{1}{\sqrt{N+1}} \sum_{k=0}^{N} \mathrm{e}^{\mathrm{i}k\varphi_o} \Phi^{(\mathrm{HG})}_{m_o+pk,n_o+qk,l_o+sk}(x,y,z) \tag{2}$$

with

$$\Phi^{(\mathrm{HG})}_{m,n,l}(x,y,z) = \frac{\sqrt{2}\,w_o}{w(z)} \psi^{(\mathrm{HG})}_{m,n}(x,y,z) \exp\left[\mathrm{i}k_{m,n,l}\tilde{z} - \mathrm{i}(m+n+1)\,\theta_G\right] \tag{3}$$

and

$$\psi^{(\mathrm{HG})}_{m,n}(x,y,z) = \frac{1}{\sqrt{2^{m+n}\pi\; m!\, n!}} H_m\left[\frac{\sqrt{2}\,x}{w(z)}\right] H_n\left[\frac{\sqrt{2}\,y}{w(z)}\right] \mathrm{e}^{-\frac{x^2+y^2}{w(z)^2}}, \tag{4}$$

where $\tilde{z} = z + [(x^2 + y^2)z] / [2(z^2 + z_R^2)]$, $k_{n,m,l} = 2\pi f_{n,m,l}/c$, and $f_{n,m,l}$ is the eigenfrequency of the cavity mode. In experiment, the phase factor ϕ_o can be determined by the far-field transverse pattern. In terms of the wave function $\Psi = \Psi^{p,q}_{m_o,n_o}(x,y,z)$, the transverse momentum density is given by [19]

$$\mathbf{g}(x,y) = \frac{\varepsilon_o}{2\omega} \mathrm{Im}(\Psi^* \nabla_t \Psi) \tag{5}$$

where ∇_t is the transverse gradient operator. Figure 6 shows calculated results for transverse patterns and transverse momentum densities varying with propagation direction from $z = 2$ mm to $z = 12$ mm for the cases of $(p, q) = (-1, 5)$ and $(p, q) = (3, 1)$, where the beam waist is at $z = 0$ mm. To satisfy the experimental far-field patterns, the phase factor ϕ_o is found to be π and 0 for the cases of $(p, q) = (-1, 5)$ and $(p, q) = (3, 1)$, respectively. Numerical results can be found to be in good agreement with experimental results for the propagation evolution of transverse patterns shown in figure 5. Moreover, the

vortex structures can be clearly seen in the transverse momentum densities.

4. Conclusions

In summary, we have employed a lowly Nd-doped YVO_4 laser with the off-axis pumping scheme to scale up the average output power of Lissajous structured beams. Experimental results that the output transmission not only influences the average output power but also significantly affects the spatial coherence. When the output transmission is greater than 5%, the spatial coherence is found to be considerably decreased and the transverse patterns become a feature of broken Lissajous figures. The optimal values for the output transmission are found to be in the range of 1.8–5.0% for making a balance between the output efficiency and the spatial coherence. Moreover, we have clearly measured the transverse patterns varying with propagation direction to manifest the 3D characteristics of Lissajous structured beams. The formula of coherent states is used to make a comparison with experimental results and to display the transverse momentum density of Lissajous structured beams varying with propagation direction. The achievement of watt-level average output power is believed to be practically valuable for utilizing Lissajous structured beams in further applications.

Acknowledgments

This work is supported by the National Science Council of Taiwan (Contract No. NSC-100-2628-M-009-001-MY3).

References

[1] Herriott D R and Schulte H J 1965 Folded optical delay lines *Appl. Opt.* **4** 883
[2] Chen Y F, Huang K F and Lan Y P 2003 Spontaneous transverse patterns in a microchip laser with a frequency-degenerate resonator *Opt. Lett.* **28** 1811
[3] Chen Y F, Lan Y P and Huang K F 2003 Observation of quantum–classical correspondence from high-order transverse patterns *Phys. Rev.* A **68** 043803
[4] Chen Y F, Lu T H, Su K W and Huang K F 2006 Devil's staircase in 3D coherent waves localized on Lissajous parametric surfaces *Phys. Rev. Lett.* **96** 213902
[5] Lu T H, Lin Y C, Chen Y F and Huang K F 2009 Observation and analysis of coherent optical waves emitted from large-Fresnel number degenerate cavities *Opt. Express* **17** 2007
[6] Lu T H, Lin Y C, Chen Y F and Huang K F 2008 3D coherent optical waves localized on trochoidal parametric surfaces *Phys. Rev. Lett.* **101** 233901
[7] Chen Y F, Lin Y C, Huang K F and Lu T H 2010 Spatial transformation of coherent optical waves with orbital morphologies *Phys. Rev.* A **82** 043801
[8] Chen Y F 2011 Geometry of classical periodic orbits and quantum coherent states in coupled oscillators *Phys. Rev.* A **83** 032124
[9] Gahagan K T and Swartzlander G A Jr 1996 Optical vortex trapping of particles *Opt. Lett.* **21** 827–9
[10] Dienerowitz M, Mazilu M, Reece P J, Krauss T F and Dholakia K 2008 Optical vortex trap for resonant confinement of metal nanoparticles *Opt. Express* **16** 4991
[11] Macdonald M P, Spalding G C and Dholakia K 2003 Microfluidic sorting in an optical lattice *Nature* **426** 421
[12] Toyoda K, Miyamoto K, Aoki N, Morita R and Omatsu T 2012 Using optical vortex to control the chirality of twisted metal nanostructures *Nano Lett.* **12** 3645
[13] Toyoda K, Takahashi F, Takizawa S, Tokizane Y, Miyamoto K, Morita R and Omatsu T 2013 Transfer of light helicity to nanostructures *Phys. Rev. Lett.* **110** 143603
[14] Molina-Terriza G, Torres J P and Torner L 2007 Twisted photons *Nature Phys.* **3** 305
[15] Gibson G, Courtial J and Padgett M J 2004 Free-space information transfer using light beams carrying orbital angular momentum *Opt. Express* **12** 5448
[16] Jesacher A, Fürhapter S, Bernet S and Marte M R 2006 Spiral interferogram analysis *J. Opt. Soc. Am.* A **23** 1400
[17] Chen Y F, Lu T H and Huang K F 2008 Spatial morphology of macroscopic superposition of 3D coherent laser waves in degenerate cavities *Phys. Rev.* A **77** 013828
[18] Chen Y F 1999 Design criteria for concentration optimization in scaling diode end-pumped lasers to high powers: Influence of thermal fracture *IEEE J. Quantum Electron.* **35** 234–9
[19] Jackson J D 1999 *Classical Electrodynamics* (New York: Wiley) chapter 6